Coastal Engineering 87 (2014) 97–111

Contents lists available at ScienceDirect

Coastal Engineering

journal homepage: www.elsevier.com/locate/coastaleng

Beach response to wave energy converter farms acting as coastal defence

Edgar Mendoza [a,*], Rodolfo Silva [a], Barbara Zanuttigh [b], Elisa Angelelli [b], Thomas Lykke Andersen [d], Luca Martinelli [c], Jørgen Quvang Harck Nørgaard [d], Piero Ruol [c]

[a] Instituto de Ingeniería, Universidad Nacional Autónoma de México, Cd. Universitaria, 04510 D.F., Mexico
[b] University of Bologna, DICAM, Viale Risorgimento 2, 40136 Bologna, Italy
[c] University of Padova, Dept. ICEA, Via Ognissanti 39, 35129 Padova, Italy
[d] Aalborg University, Dept. of Civil Engineering, Sohngaardsholmsvej 57, DK-9000 Aalborg, Denmark

ARTICLE INFO

Article history:
Received 1 July 2013
Received in revised form 14 October 2013
Accepted 18 October 2013
Available online 12 November 2013

Keywords:
Wave energy converters
Coastal protection
Coastline response
Wave transmission
Numerical modelling

ABSTRACT

One of the greatest challenges of coastal engineering today is the need for coastal protection in the changing climate scenario. Places which are nowadays protected will demand upgraded defences and more sites will require security; in all cases a large amount of resources will be needed to ensure beach maintenance and coastal safety. This may be an opportunity for the multi-purpose use of Wave Energy Converters (WECs) if the foreseen increase of energy demand in coastal areas is also considered. In this paper a group of WECs based on different operating concepts is numerically tested in front of two beaches, i.e. the Bay of Santander in Spain and Las Glorias beach in Mexico, representing two different case studies where the long-shore sediment transport is dominant. The hydrodynamics induced by these devices is represented by means of a 2D elliptic modified mild-slope model that is calibrated against new experimental results. The wave field is then used as input for the analytical calculation of the long-shore sediment transport and the coastline trend is estimated by applying the continuity of sediment equation. The characteristics of the selected numerical models give this work a first approach level. All the devices were found to produce a positive trend (accretion) at least in small areas. Recommendations are given to facilitate the selection of the device and the design of the farm layout for shore protection purpose.

1. Introduction

The expected increase in number and intensity of storms due to climate change, the present situation of coastal areas already severely exposed to erosion and flooding together with the need to preserve coastal ecosystems in a way acceptable to societies point the way for careful, long-term, innovative coastal defence strategies. Nourishment alone is one of the preferred protection techniques; however experience has already shown that its efficiency and lifetime is considerably increased when the shore is protected by hard defences. Also, local sand resources are limited, leading in many cases to the search for alternative sites for borrowed sand areas (off-shore deposits, dredging from river mouth and harbour entrance). As far as is possible, the hard defences should be climate proof (i.e. characterized by low sensitivity to sea level rise), environmentally friendly (i.e. constructed with eco-compatible materials) and eventually characterized by low visual impact on the horizon (i.e. submerged or low-crested).

Moreover, economic and social growth in coastal areas in the recent past, suggests that the local energy demand will continue to grow and lead to an increase of anthropogenic stressors on top of the climatic and environmental sources of threat. The sea space in particular may be subject to additional installations for aquaculture, exploitation of renewable energy, oil and gas, transportation, etc. Among these installations, Wave Energy Converters (WECs) are particularly interesting since they partially absorb waves in producing electricity and may thus reduce the wave energy incident on the littoral. It is, however, undeniable that implementation of many of the small scale WECs developed and scale tested worldwide is still far from being considered a reality as construction, operation and maintenance costs compared to the economic recovery times make them unaffordable.

The combination of these observations prompted the idea that the THESEUS project investigates a systematic way of using floating WECs for coastal protection. The concept of WECs as multipurpose structures may be a win–win alternative, making feasible the implementation of proven and newly developed devices and, at the same time, obtaining a certain degree of beach protection, although this will be limited by the specific features of the WEC (installation depth, layout of the array, etc).

So far the hydrodynamic performance of large parks of WECs and therefore their optimal mutual placement for energy absorption has been studied mainly through numerical models, Folley et al. (2012). This leads us to suppose a possible limitation; although a WEC farm can be used as coastal defence it has to be placed where it finds its optimal efficiency and this is not necessarily the best location for coastal protection, so a comparison between the performance of WECs as costal

* Corresponding author at: Circuito Escolar s/n, Edificio 5, Cubículo 408, Instituto de Ingeniería, Ciudad Universitaria, 04510, Coyoacán, DF, México. Tel.: +52 55 56233600x8632; fax: +52 55 56162798.
E-mail address: emendozab@ii.unam.mx (E. Mendoza).

0378-3839/$ – see front matter © 2013 Elsevier B.V. All rights reserved.
http://dx.doi.org/10.1016/j.coastaleng.2013.10.018

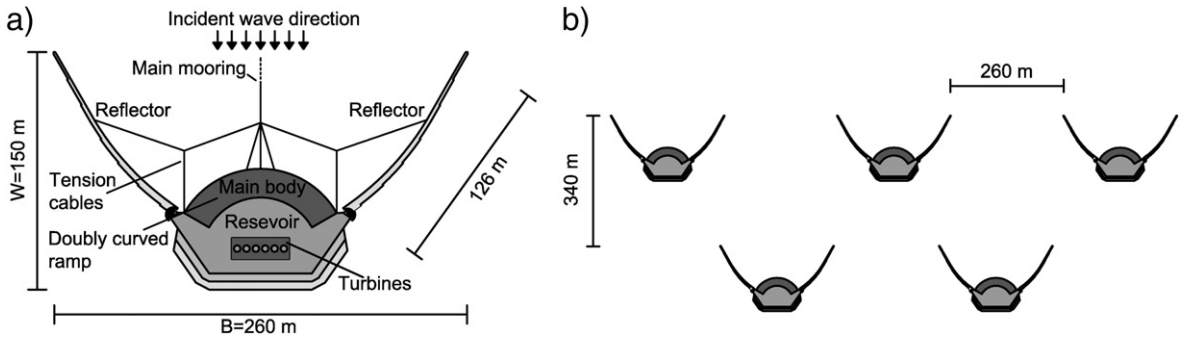

Fig. 1. a) Overall dimensions of the 24 kW/m WD-model. b) Distances between individual devices when positioned in a staggered grid.

defence and traditional alternatives would be unfair because of these spatial constraints.

The concept of the park effect dates back to 1980, when the pioneers Budal (1977), Evans (1979) and Falnes (1980) analytically studied the use of heaving axisymmetrical WECs under regular and unidirectional waves. Similar studies, i.e. following the linear potential flow theory, have been recently proposed by Child and Venugopal (2007) and by Garnaud and Mei (2009). However this approach is not applicable under irregular wave conditions or in the case of devices with Multiple Degrees of Freedom.

More realistic numerical codes are based on the boundary elements methods (BEM), such as WAMIT, ANSYS Aqwa, Aquaplus, etc. Examples of BEM calculation can be found for arrays of heaving point absorbers by Ricci et al. (2007) and floating Oscillating Surge Converters by Borgarino et al. (2011). However even the BEM codes have limitations, mainly related to the constraints of the uniform water depth, to the high CPU requirement and to their inability of modelling viscous effects directly, Li and Yu (2012).

Boussinesq and spectral wave models are designed for wave propagation over large domains accounting for sea bottom effects. The main limitation of these models is the impossibility to intrinsically simulate moving structures. WECs have been represented as porous layers with a given reflection/transmission coefficient by Millar et al. (2007), Venugopal and Smith (2007) and by Mendes et al. (2008). Beels et al. (2010) performed numerical modelling of WEC farms using mild-slope wave propagation models and sponge layer technique and Folley and Whittaker (2010), developed a spectral model to evaluate the performance of WECs.

The most significant conclusions from the numerical modelling of WECs were reviewed by Babarit (2013) in the form of guidelines for WEC farm layout. In particular, for small devices (whose typical long-shore dimension, B, is 10–20 m) deployed in small arrays (up to 20 devices), with a mutual distance around 10–20 B it is suggested that they be placed in limited number of wave farm lines. It is worth noting that the main target of most studies related to WECs is the generation of power by such installations. Therefore the wave farm design does not take into account secondary goals, for instance: the narrower the gap width the higher the wave absorption and therefore the lower the wave transmission; for information on the accessibility of the offshore wind farm in the lee of a WEC farm, the reader is referred to Beels et al. (2011).

Within the THESEUS project, four different WECs were studied as near-shore protection alternatives. These WECs included an overtopping device (Wave Dragon, www.wavedragon.net), multi-oscillating water-column device (Seabreath, www.seabreath.it), wave activated bodies (DEXA, www.dexawave.com), and a new concept (Blow-Jet). The wave transmission curve for a single device was experimentally derived (Nørgaard and Lykke Andersen, 2012; Ruol et al., 2011a; Zanuttigh et al., 2013) and the hydrodynamic interaction of multiple devices when placed in farms was numerically modelled (Angelelli and Zanuttigh, 2012; Nørgaard and Lykke Andersen, 2012).

Little attention has been paid so far to the response of the coastline in the presence of WECs. To the authors' knowledge, only Millar et al. (2007) studied the shoreline change due to a generic wave farm while Zanuttigh et al. (2010) and Ruol et al. (2011b) analysed the effects of a DEXA device on the long-shore sediment transport at a specific location.

The aim of this paper is to systematically analyse the performance of the same WECs examined in THESEUS in terms of coastal protection and to estimate the induced shoreline change. This analysis is performed numerically in a homogeneous way for all the devices, through the 2D porous mild-slope model from Silva et al. (2006).

More specific objectives of this paper are: to evaluate the coastline response to the modified wave field around the WEC farms and to provide the reader with design criteria for WEC installations for coastal protection.

In Section 2 a brief description of the devices is presented together with highlights of the transmission coefficient functions. Section 3 describes the study sites as well as the design of the WEC farm layout. It also shows the results of the 2D wave propagation model. The numerical model for the evaluation of the coastline response and its results are the object of Section 4 and the over-all conclusions are given in Section 5.

2. Description of the WEC devices

2.1. The Wave Dragon

In Nørgaard and Lykke Andersen (2012) the use of different concepts of Wave Energy Converters (WECs) for the combination of electricity production and coastal protection is discussed. One of the promising concepts is the Wave Dragon (WD) due to its size and large

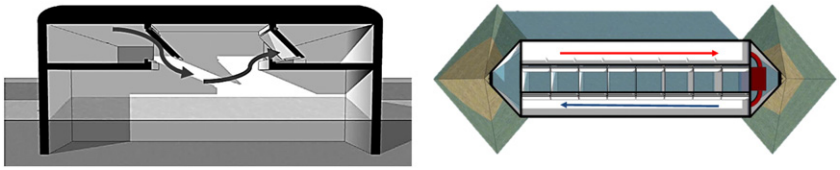

Fig. 2. Cross-section (left) and plan view (right) of Seabreath.

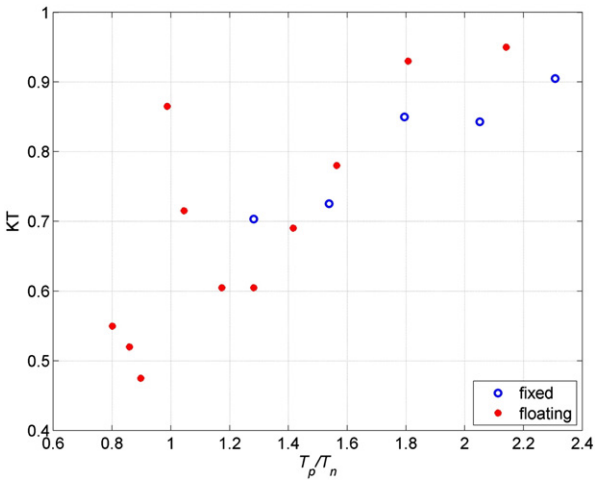

Fig. 3. 1:100 scale tests results for Seabreath with irregular waves.

wave absorption capacities. Additionally, since it is a floating structure, the WD is not sensitive to sea water level rise due to climate change.

The WD consists of two so-called wave-reflectors which guide the wave energy onto a doubly curved ramp on the so-called main body where the waves overtop into a reservoir. The overall dimensions of the 24 kW/m model (i.e. specifically developed for the North Sea) are illustrated in Fig. 1a). Electricity is produced when the stored water potential in the reservoir drains back into the sea through a number of turbines. The WD is moored using a single cable and is thus able to turn and face the incident wave direction. Tension cables are used to stabilize the reflectors. It is desirable to position WDs in farms of multiple devices to reduce costs. In order to avoid collisions of the devices the recommended mutual distances are of the order of the device width in the long-shore direction and of one and a half device length in the cross-shore direction, see Fig. 1b). The spacings between the devices forming a WD farm and the shape of the resulting wake effects were studied by Beels et al. (2010).

For the Wave Dragon as presented in Nørgaard and Lykke Andersen (2012) the overall transmission coefficient is given by

$$K_{T,D} = -0.087\frac{W}{L_p} + 0.82 \qquad \textit{for} \quad 0.905 < \frac{W}{L_p} < 1.232 \tag{1}$$

where $K_{T,D}$ is the transmission coefficient, W the device width and L_p the deep water peak wave length.

As explained in Nørgaard and Lykke Andersen (2012) the overall wave transmission coefficient of a single WD (if outside of the range $0.905 < W/L_p < 1.232$) can be approximated with relatively good accuracy based on integration of wave energy flux from the draught of the device to the seabed.

2.2. The Seabreath

The Seabreath is an Italian device, patented by Luigi Rubino, inventor, www.seabreath.it, and developed with the financial support of the Merighi Group. It is an elongated structure, formed by a series of aligned rectangular chambers with an open bottom (Fig. 2). The device is aligned perpendicularly to the incident wave crests, i.e. it is of the attenuator type of WECs.

This device may be placed near-shore on piles or off-shore as a floating structure. According to the classification proposed by Thorpe in 1992 (see for instance Thorpe, 2000) the Seabreath is of the Oscillating Water Column (OWC) type, since each chamber behaves as an OWC.

When air in each chamber is compressed (wave crest), it is directed by non-return valves toward a longitudinal high pressure duct; when air is decompressed (wave through), low pressure air is directed toward a low pressure duct. The peculiar recirculation system of the device includes further details that increase performance under irregular wave conditions and allow the device to "breathe", hence the name.

A unidirectional impulse turbine connected between the high and low pressure ducts is ideally used to generate energy. Since the wave travels from one chamber to another, the induced flow is relatively steady, with consequent benefits for the turbine efficiency.

The considered device is 150 m long, 30 m wide with a 10 m draught. For the placement of devices in arrays, the investigated gap between adjacent modules has been equal to 7/3 the device width.

Since the Seabreath is an attenuator WEC, it absorbs the energy from the sides. The capture width is in fact potentially larger than the actual width, meaning that a single device may convert or dissipate more energy than the one confined in its width. In this special case, the single device may be treated as a terminator with a width equal to the capture width, and for this width $K_{T,D} = 0$. In practice, for the artificial definition of the effect of a single device in the numerical model, the transmission coefficient is estimated in two steps. First, an empirical value, K_T, is taken from the 1:100 scale tests results which are presented in Fig. 3 relative to an array with 70% of voids; the second step is to substitute K_T in the equation for $K_{T,D}$:

$$K_T^2\frac{10}{3}b = K_{T,D}^2 b + 1^2\frac{7}{3}b, \textbf{\textit{i.e.}} K_{T,D}^2 = \left(\frac{K_T^2 - 0.7}{0.3}\right) \tag{2}$$

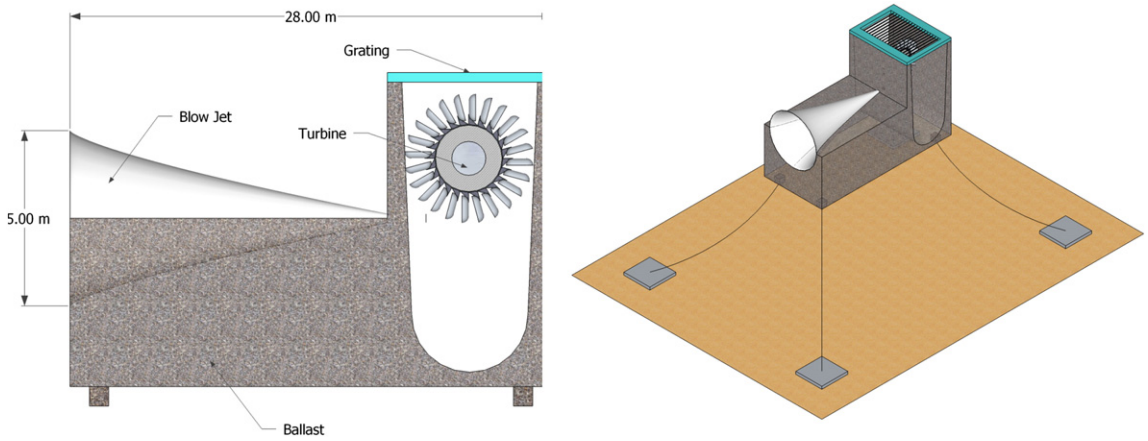

Fig. 4. Cross (left) and isometric (right)views of the Blow-Jet.

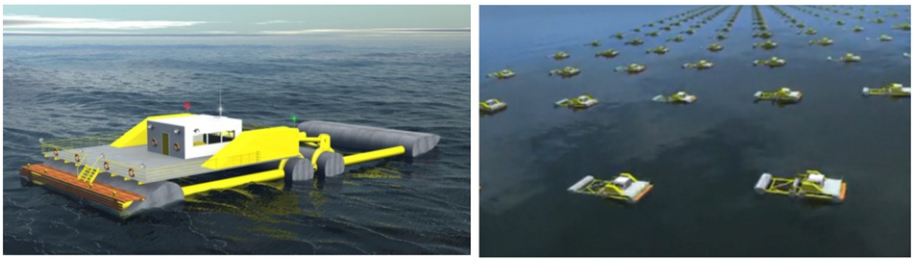

Fig. 5. The DEXA concept (left) and an example of a DEXA wave energy farm (right, www.dexawave.com).

where b is the device width and the interaxis between devices is 10/3 b. If $K_{T,D}^2$ is complex, then a different equation should be used, aiming at finding the fictitious device width b' to be associated to a null $K_{T,D}^2$:

$$K_T^2\frac{10}{3}b = 0^2b' + 1^2\left(\frac{10}{3}b - b'\right), \boldsymbol{i.e.}\, b' = \frac{10}{3}b\left(1-K_T^2\right) \tag{3}$$

The device is assumed as not modifying the wave period and, as the water level before and after the device is similar, the energy balance used to derive the transmission coefficient expressions does not depend on the group celerity.

2.3. The Blow-Jet

This device aims to reproduce the hydraulic behaviour of the well-known, naturally occurring blowholes, the most famous example on the Mexican coast being the so-called "Bufadora" in Ensenada, Baja California.

The complex internal morphology of blowholes has been poorly studied so far. This natural formation always presents a catchment entrance, a compression cavern and an expelling hole. The different sizes, slopes and arrangement of these three components determine the force and air–water mixture of the expelled jet.

The Blow-Jet is a floating WEC which converts energy by directing the expelled jet to a turbine. The overall dimensions of the device considered in this study are shown in Fig. 4. The simplicity of the shape of the Blow-Jet poses few restrictions to the array layout. The one considered for this study is in modules of three cones, giving a total width of 45 m and a length of 28 m for each module. The long- and cross-shore gaps between modules are defined by 1.5 times the corresponding device dimension.

The function that describes the transmission coefficient for a single Blow-Jet is

$$K_{T,D} = 0.084\left(\frac{P}{L_p} - 0.0049\right)^{-0.55} \quad \textbf{\textit{for}}\ 0.02 < \frac{P}{L_p} < 0.22 \tag{4}$$

where P is the draught and L_0 the deep water peak wave length.

2.4. The Dexa

The DEXA device (see Fig. 5) consists of two rigid pontoons with a hinge in between, which allows each pontoon to pivot in relation to the other. The draught is such that at rest the free water surface passes along the length of the axis of the four buoyant cylinders. The Power Take-Off (PTO) system consists of low pressure power transmission technology and is placed close to the centre of the system, in order to maximize the stabilization force (Kofoed, 2009).

The Dexa dimensions at prototype scale were designed for the North Sea as with the Wave Dragon; the device is expected to be 60 m long and 24 m wide.

The transmission coefficient for a single Dexa device is

$$K_{T,D} = -0.276\left(\frac{W}{L_p}\right)2 + 0.4304\left(\frac{W}{L_p}\right) + 0.6781 \quad \textbf{\textit{for}}\ 0.49 < \frac{W}{L_p} < 1.26 \tag{5}$$

Where W is the device width and L_p the deep water peak wave length.

In Eqs. (1) to (5) only the transmission coefficient functions for a single device are presented; given that the devices will be placed separately in the numerical model, the effects of multiple devices will be calculated by the wave propagation model.

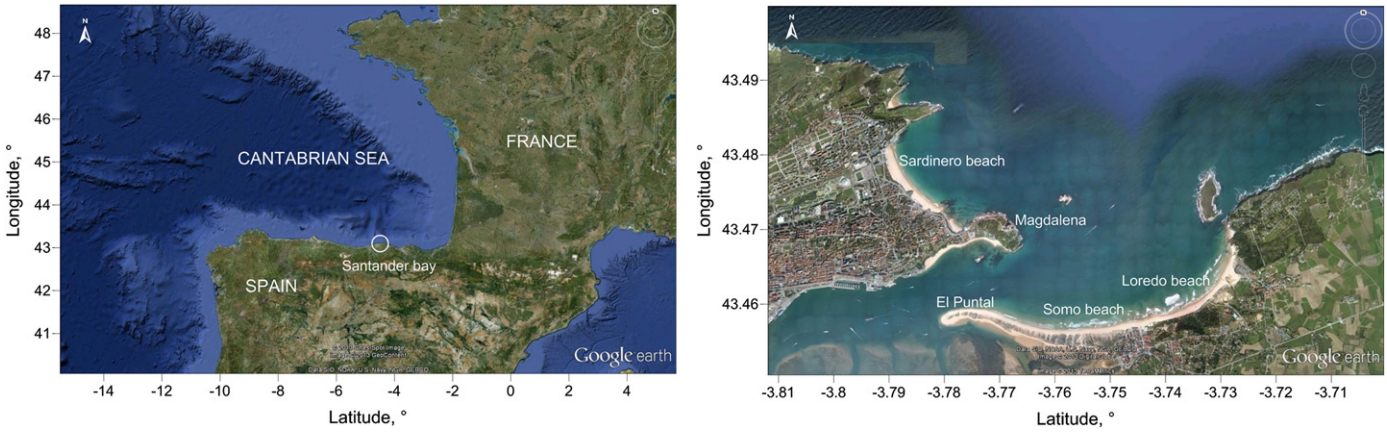

Fig. 6. Location of Santander Bay (left) and beaches of interest (right), (Google Earth, 2013).

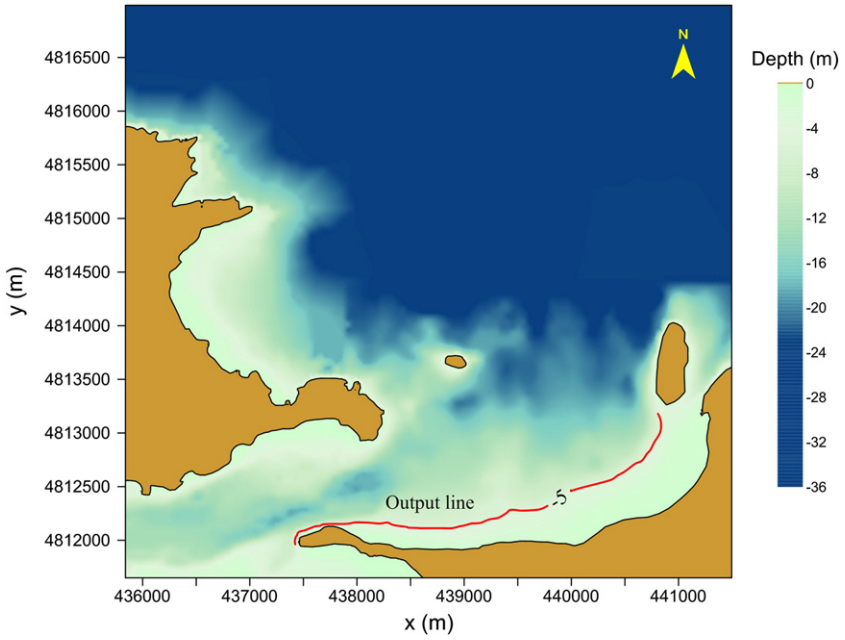

Fig. 7. Present bathymetry of Santander Bay.

Table 1
Representative wave conditions for Santander Bay.

Case	Hs, m	Tp, s	Spectrum type	Gamma	Smax	Principal direction from North	Spreading function
S1	4.0	8	TMA	3.3	10	45° counterclockwise	Mitsuyasu
S2	4.5	10	TMA	3.3	10	22.5° clockwise	Mitsuyasu

3. Case studies

Two different study sites were selected aiming at comparing the effects on the two coastlines: a semi-closed water body and a straight beach. It is relevant to note that each device has different installation requirements so not all the devices can be placed in the same site because a balance has to be found between the minimum reasonable energy production and the degree of shore protection needed. The following sub-sections describe the sites and how the modelled farms were defined.

3.1. Santander Bay, Spain

Santander Bay on the Cantabrian coast in the North of Spain (Fig. 6 left) was selected as the first case study because it is a large semi-closed water body with high energetic waves. In addition, Santander is an important touristic, industrial and economic city where shore protection is needed as demonstrated by the flooding registered there in the 2010–2011 winter. The study aims to evaluate the possibility of protecting with WEC farms the sand spit known as El Puntal and Somo and Loredo beaches in the South and East, respectively (see Fig. 6 right).

The wave climate of Santander Bay is governed almost all year by waves coming from the NW with high variability of periods which include mean and extreme conditions; some smaller waves are reported to come from the NNE (www.puertos.es). The mean tidal range at Santander is 3 m while the spring tidal range is 5 m (Medellin et al., 2008).

The hydrodynamic performance of the WECs is investigated under both of these wave directions to give an indication of the different effects on the coastline. Since the devices studied in this paper are floating, the tidal variations have a very limited influence on the WECs performance.

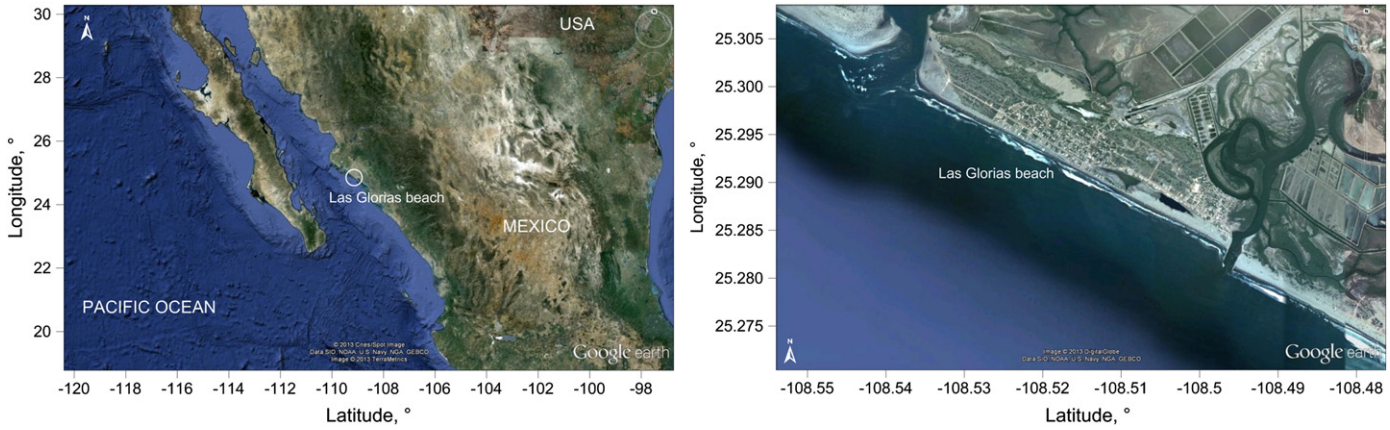

Fig. 8. Location of Las Glorias Beach (left) and detailed view of the site (right).

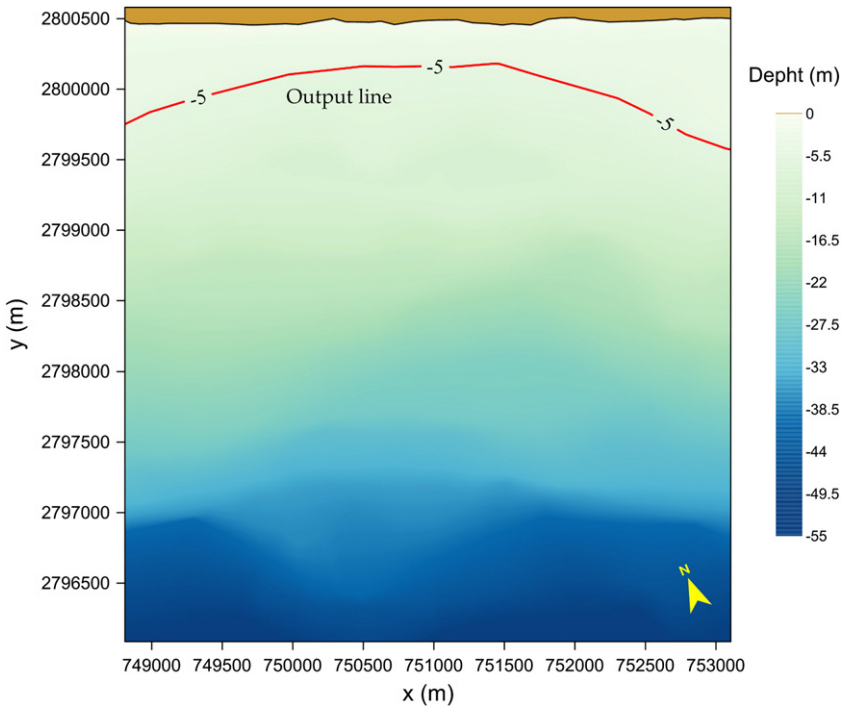

Fig. 9. Present bathymetry of Las Glorias Beach.

The present bathymetry of Santander Bay is shown in Fig. 7 together with the output line that will be used to evaluate the performance of the WEC farms. The main characteristic of this site is that relatively deep waters can be found close to the limits of the bay in the sea side, which is favourable for the WECs placement.

The wave conditions selected as representative and that were used in the numerical modelling are listed in Table 1.

In average the S1 case can be found 30 h a year and case S2 occurs 744 h a year.

3.2. Las Glorias Beach, Mexico

Las Glorias Beach is located on the North Pacific coast of Mexico inside the Gulf of California (Fig. 8 left). This site is of interest because it presents a short fetch with short wave periods and small wave heights, with the exception of waves coming from the South which are more energetic. As can be seen in the right panel of Fig. 8, the beach is limited to the North and to the South by rivers. Two groynes were built, for navigation purposes, in the South of the river mouth which blocked the Northward directed longshore sediment transport and caused a coastline retreat of about 150 m (Zayas, 2012) reducing dramatically the resilience of the littoral system and exposing the population to high risk of erosion and flooding. The need for mitigation measures, mainly wave energy dissipation is evident. Las Glorias is a straight beach approximately 4 km long; thus for analysing the hydrodynamics and beach response induced by the WEC farms; it will be divided into North, Central and South beaches.

Table 2
Selected wave conditions for Las Glorias Beach.

Case	Hs, m	Tp, s	Spectrum type	Gamma	Smax	Principal direction from North	Spreading function
G1	3.0	4.5	TMA	3.3	10	180°	Mitsuyasu
G2	3.0	7.0	TMA	3.3	10	180°	Mitsuyasu

The wave climate at Las Glorias is dominated by small waves coming from W and SW but also every year during Summer and Autumn waves with periods from 4 to 8 s come from South (Silva et al., 2008); the latter being the worst condition for beach erosion as it generates greater sediment transport. The tidal variation in this site can be neglected (microtidal regime).

The present bathymetry of Las Glorias is illustrated in Fig. 9.

Using the worst case scenarios for beach erosion, the wave conditions coming from the South were selected for numerical modelling which are presented in Table 2.

Waves coming from the South at Las Glorias (cases G1 and G2) occur, in average, 50 h a year.

In both cases, TMA spectrum has been chosen as the wave propagation begins in intermediate waters for longer periods.

3.3. Design layout of the WEC farms

As described in Section 2, the WEC devices considered in this paper have very different concepts and optimal operation conditions. As a result, their sizes, minimum required depths and wave climate ranges of operation are highly uneven. This leads to the situation that although a floating structure can be placed almost anywhere by adjusting its

Table 3
Installation characteristics of the WEC devices in Santander Bay.

	Wave Dragon	Blow-Jet
Minimum water depth (m)	30	15
Cross shore dimension (m)	150	28
Long shore dimension (m)	260	45
Long shore gap width (m)	260	67.5
$K_{T,D}$ per one device	0.73 Eq. (1)	0.47 Eq. (4)
No. of devices 1st line	2	8
Long shore farm dimension (m)	780	832.5
Cross shore farm dimension (m)	500	28
Number of lines	2	1
Overall K_T	0.75	0.77

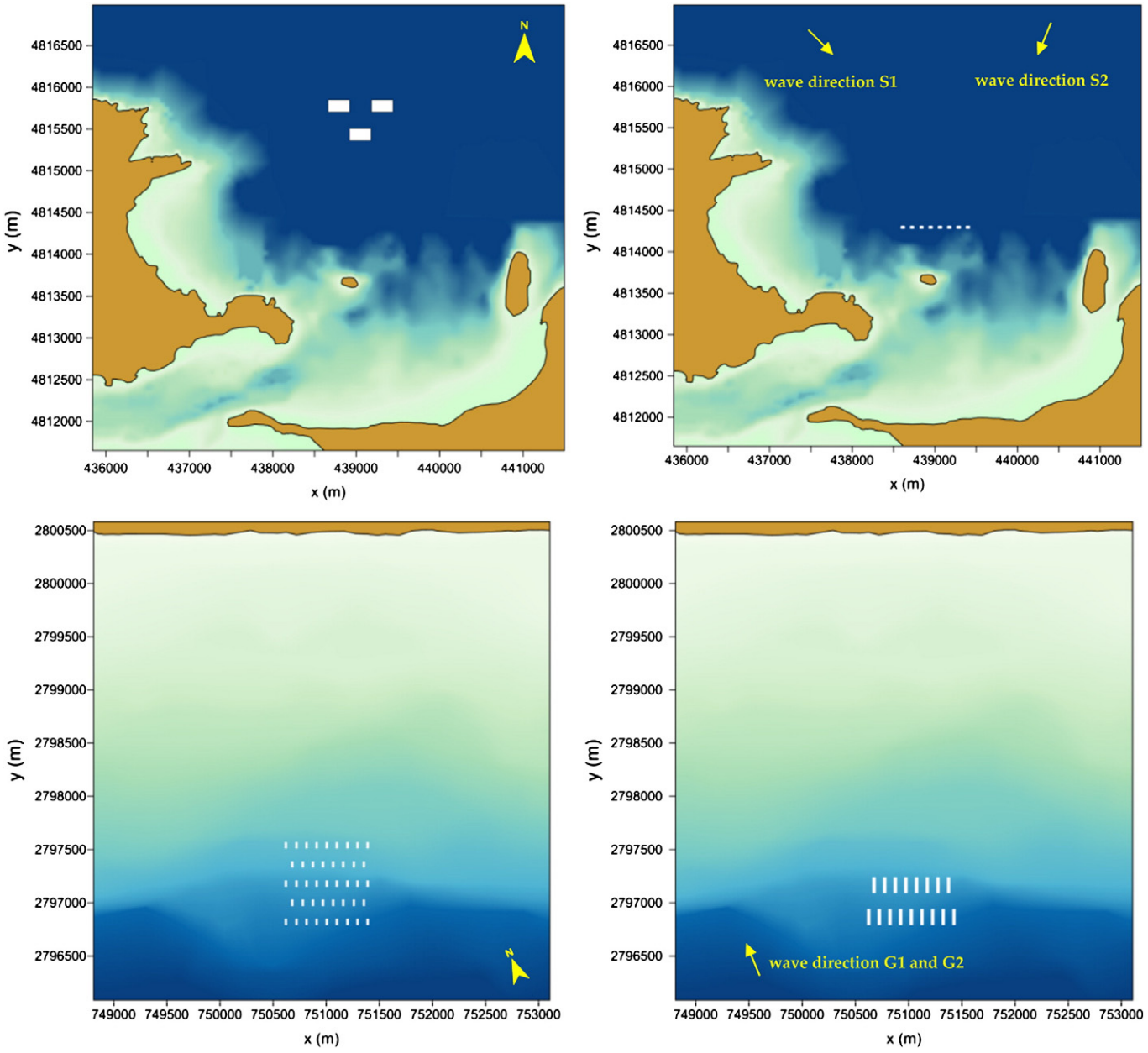

Fig. 10. WEC farm layouts for Wave dragon (top left), Blow-Jet (top right), Dexa (bottom left) and Seabreath (bottom right).

dimensions, when the structure is a WEC there has to be a compromise between its operation and its energy production capabilities. This means that a device cannot be freely adjusted to whichever site, instead, the hydrodynamic (e.g. wave length) and morphological characteristics of the site must be taken into account to select and tune the device so that, while generating energy properly, it is capable of offering the needed coastal protection. In this sense, to evaluate and compare the performance of the devices under study, each of them was placed in the site that best suited their installation requirements and using the dimensions recommended by the developers (see Section 2). The energy production of each device is beyond the scope of this paper.

The design of the WEC farms for coastal protection was aimed at obtaining

- the same target protection level, i.e. a target transmission coefficient of 0.7–0.75; this value was selected by comparison with low crested breakwaters (Van der Meer et al., 2005);
- the protection of the same area; the number of devices of the first line of the farms was determined so that approximately the same long-shore distance was covered.

Based on the device dimensions and on their operating principle, a suitable depth for installation was chosen. The distances between the devices was decided taking into account the device motions detected

Table 4
Installation characteristics of the WEC devices in Las Glorias Beach.

	Dexa	Seabreath
Minimum water depth (m)	30	20
Cross shore dimension (m)	60	150
Long shore dimension (m)	24	30
Long shore gap width (m)	120	70
$K_{T,D}$ per one device	0.83 Eq. (5)	0.79 Eq. (2)
No. of devices 1st line	9	9
Long shore farm dimension (m)	792	830
Cross shore farm dimension (m)	780	450
Number of lines	5	2
Overall K_T	0.70	0.63

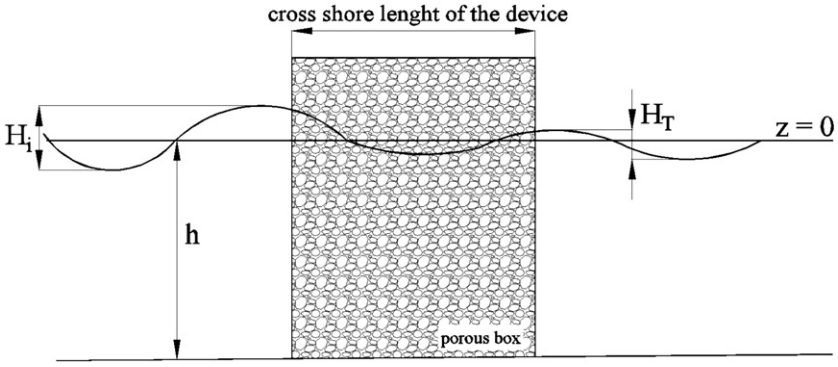

Fig. 11. Fluid definition of the 1D mild-slope model.

Table 5
Equivalent porous boxes (porosity, *E* and friction, *F*) for WECs derived from the calibration of the 1D numerical model.

Device	*F*	*E*	$K_{T,D}$ computed
Wave Dragon	0.0150	0.62	0.73
Blow-Jet	0.0050	0.40	0.47
Dexa	0.0016	0.60	0.81
Seabreath	0.0013	0.48	0.81

during the experiments and the space required for realistic mooring systems. The wider the long-shore gaps, the lower the coastal protection level and the lower the device density and, therefore, the lower the energy production compared to the same occupied marine space ratio. The Seabreath is the only device of the attenuator type, therefore offering the advantage of much narrower long-shore gaps than the other devices.

The staggered configuration of the devices gives the best performance for both coastal protection and energy production. It maximises the wave energy approaching the lines inshore of the first one and also

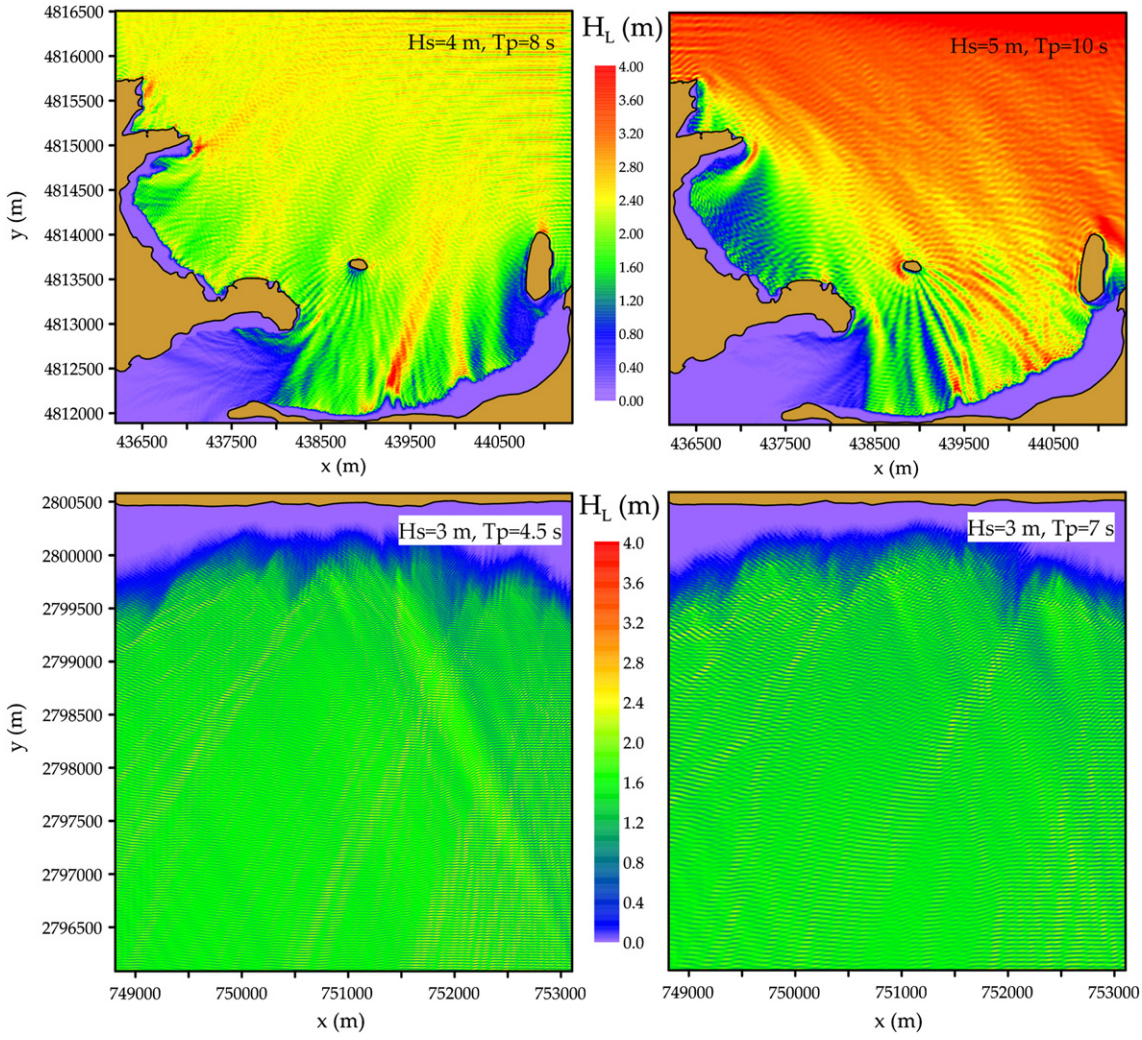

Fig. 12. Present conditions for Santander Bay (top) and Las Glorias Beach (bottom), cases S1 and G1 are presented in the left column and S2 and G2 in the right column.

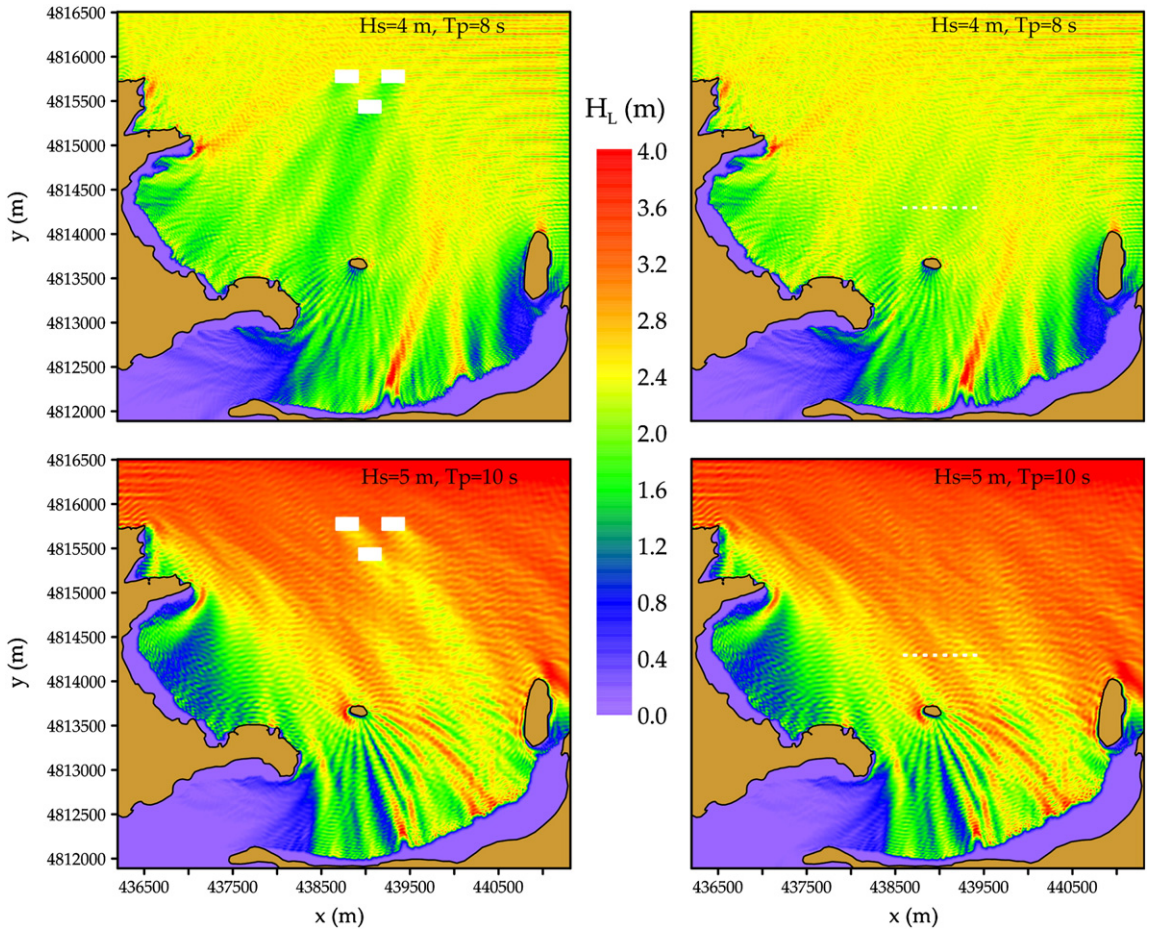

Fig. 13. Maximum wave height maps for Santander Bay, Wave Dragon (left column) and Blow-Jet (right column), the upper line presents case S1 while case S2 is displayed in the bottom line.

maximises the density of the devices in the cross-shore direction, therefore leading to the best configuration for energy production. At the same time, this configuration avoids the presence of completely unprotected gaps and may lead to a further decrease of the wave height behind the farm, thus exploiting a constructive interaction between the devices in the same farm line.

Although the devices are considered as floating, the obstacle they represent to the wave propagation will necessarily produce wave diffraction, which may reduce the wave energy in some areas but increase it in others, so the energy distribution has to be carefully tracked in order to avoid undesired effects on beaches or navigation routes. On the other hand, the interaction of waves in the space between the devices strongly depends on the distance between them; considering this, the separation proposed herein is large enough to avoid resonance effects; which is also beneficial for the consecutive farm lines, as chaotic waves are thus avoided.

3.3.1. Layout of the WEC farms at Santander Bay

The concept under which Blow-Jet and the Wave Dragon were developed allows their implementation in sites with large wave periods; thus the proposal of this study is to place them in Santander Bay. The prototype dimensions followed those suggested by the developers (see Section 2).

The conditions selected for the design and optimisation of the WECs and the farms at Santander Bay correspond to case S2 in Table 1. A summary of the installation characteristics obtained is presented in Table 3, where it can be seen that similar overall transmission coefficients can be reached with different device numbers, in general, the same marine area has been covered.

The Wave Dragon farm seems to have relatively few devices, but as it absorbs high wave energy and it is placed in deeper waters its effect on the coast is expected to cover a larger area of the coast than the Blow-Jet which is closer to the beach. In turn, the Blow-Jet farm also has few devices but as the computed transmission coefficient for a single device is small, the overall target K_T is reached with only one line of devices. The defined farm layouts for Wave Dragon and Blow-Jet are shown in Fig. 10.

3.3.2. Layout of the WEC farms at Las Glorias Beach

In the case of Seabreath and Dexa, as their development concept and optimal operation is found at low periods, this study considers placing them to protect Las Glorias Beach. The design of both devices, i.e. the cross-shore length, was optimised based on the local dominant peak wave length.

Dexa and Seabreath present higher single device transmission coefficients than Wave Dragon and Blow-Jet and as the gaps between devices are also large, several lines are needed to achieve the target K_T. Much more marine area is covered by these farms so their application should be in open areas, which makes them, again, suitable for Las Glorias Beach. The installation characteristics of Dexa and Seabreath farms as obtained from considering G2 wave conditions (Table 2) are shown in Table 4, while the farm layouts for Dexa and Seabreath are illustrated in Fig. 10. It should be noted that for the Seabreath case, the G2 conditions correspond to the worst possible case in terms of shoreline

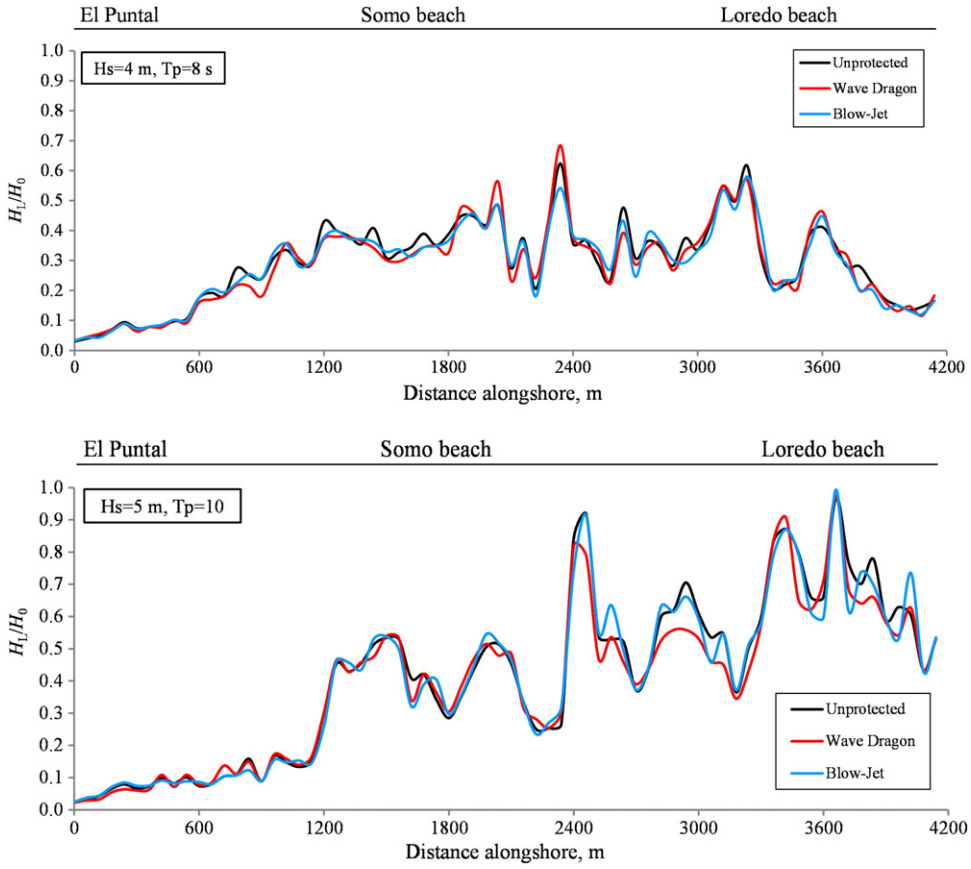

Fig. 14. Wave height reduction nearshore for Santander Bay, case S1 (top) and case S2 (bottom).

protection (close to resonance in floating conditions), although suitable in terms of energy production. For periods both larger and smaller than these, the transmission coefficient would be much smaller.

4. Modelling of the hydrodynamics induced by the wave farms

4.1. Modelling procedure and settings

The estimation of the effects induced by the presence of the WECs was carried out in two phases. In the first phase each device was represented as an infinitely high porous box but with its actual cross-shore length in the 1D elliptic mild-slope equation model by Silva et al. (2002). This is a time independent model which propagates linear waves through a single finite, homogeneous and isotropic porous media. A typical cross-section of the fluid domain is shown in Fig. 11.

The characteristic porosity and internal friction of the boxes was calibrated for each device, as a function of the peak period, by means of the new experimental results available. The transmission coefficients obtained from Eqs. (1) to (5) with case S2 for Wave Dragon and Blow-Jet and case G2 for Dexa and Seabreath were the target values for the 1D mild-slope equation.

The equivalent porous characteristics (porosity, *E* and friction, *F*) and the approximated transmission coefficient found via the mild-slope model for each device are summarized in Table 5.

In the second phase, the 2D modified elliptic mild-slope equation model WAPOQP by Silva et al. (2006) modified to run spectral and multidirectional waves (irregular short-crested waves) was used to compute the wave field. This is, as well as the 1D model, a time independent, finite differences mild-slope equation model for linear waves which solves the reflection and phase coefficient shift in the porous layer implicitly. The boundaries can be set to open, partially reflecting or fully absorbing and the resulting sparse-banded matrix is solved using Gaussian elimination. The model incorporates an energy dissipation term to take into account losses from wave breaking and bottom friction.

The lateral boundaries in both case studies were set to open and the land boundaries within the domain were set to partially reflective with a coefficient of 0.3 for beach areas and 1.0 for cliffs.

The mild-slope model was selected because of its simplicity but good accuracy in first and basic approach works and decision making studies, such as the one conducted here, where it is also common to have little data available. Additionally, as the farms are located in different depths and in a variety of configurations (i.e. gaps, number of lines and number of devices) deep water calculations are needed to obtain the waves in front of the farms; non-linear models are known to lose accuracy precisely in deep water. However, Nørgaard and Lykke Andersen (2012) observed that moving devices can be modelled with good accuracy using a depth-integrated Boussinesq model. In turn, the linear models can over-estimate the length of the wake effect and its intensity as they are not capable of reproducing variations in the mean period. As a consequence the beach response may also be over-estimated; the computed trends given in this paper are intended to offer recommendations and help in decision making. For design and detail purposes, other models could be more accurate.

Before introducing the hydrodynamics induced by the WEC farms in the case study domains and in order to set a reference point, the wave fields for cases S1, S2, G1 and G2 from Table 1 and Table 2 are presented in Fig. 12.

The hydrodynamic results, beach response and discussion that follow are referred to the output lines shown in Figs. 7 and 9 which correspond to the 5 m depth line.

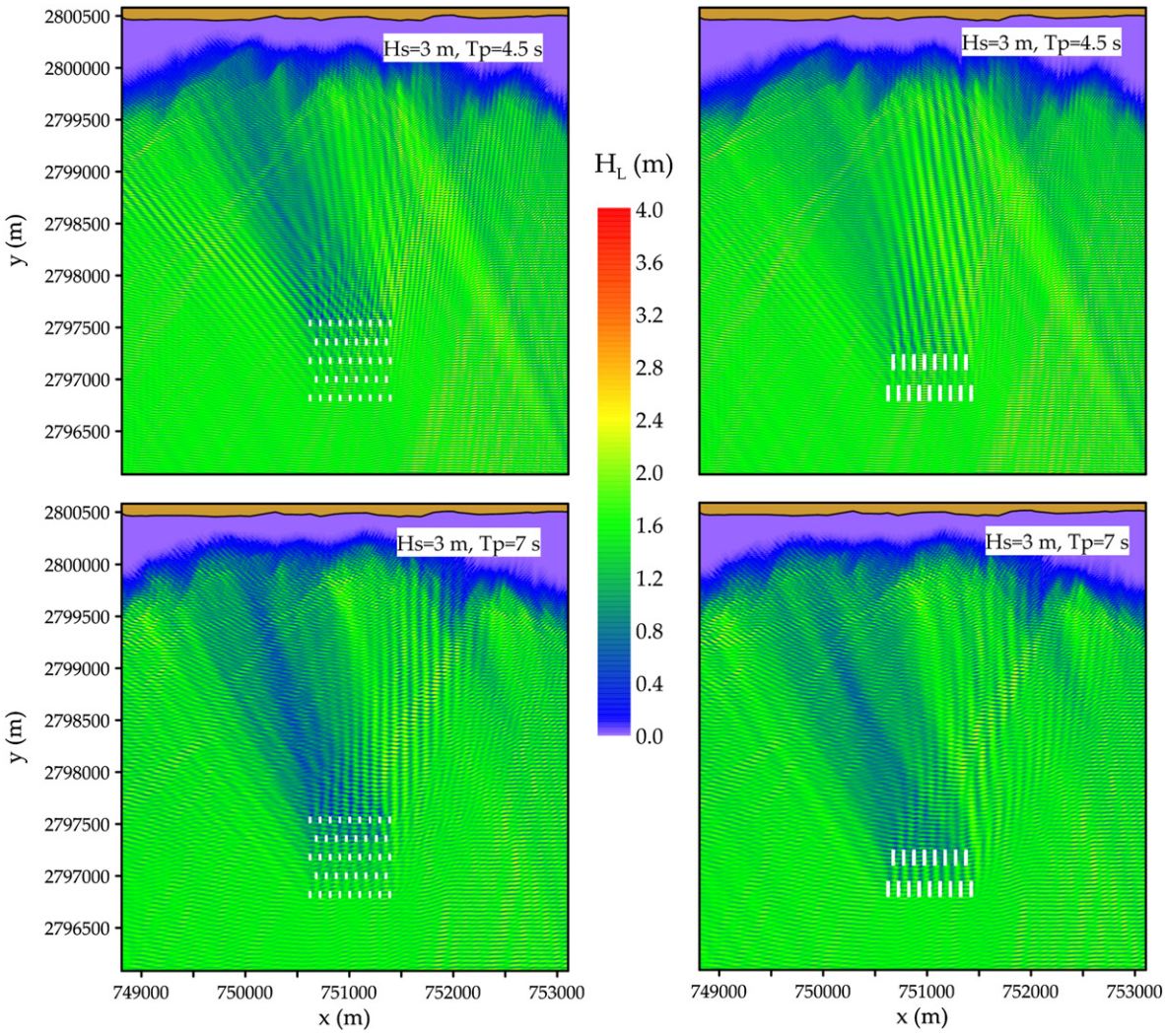

Fig. 15. Maximum wave height maps for Las Glorias Beach, Dexa (left column) and Seabreath (right column), the upper line shows case G1 results and the bottom line corresponds to the G2 case.

4.2. Hydrodynamic performance in Santander Bay

The Santander numerical domain consists of a regular mesh with squared 8 m cells, as was said before, the East and West boundaries were set to open and waves were entering from the North boundary.

Although the WEC farms occupy relatively small marine areas, the wake effect is clearly seen in the maximum wave height maps shown in Fig. 13, where the results for Santander Bay are shown.

When the Wave Dragon farm is in place, for case S1, the waves approach the Northern part of Sardinero beach without major changes. In contrast, the Southern part of this beach and the Magdalena peninsula receive approximately 10 and 15% less wave energy, respectively (the percentage is estimated based on the ratio between the present and protected wave height along the output line). The wake effect covers a small portion of Magdalena peninsula, El Puntal and a small part of Somo beach; that is, in almost 2 km of coastline wave energy reduction is found. Modelling this wave direction (S1), Loredo beach is not protected at all with the Wave Dragon farm. For the same waves (S1), the Blow-Jet, being placed in shallower areas, shows a narrower wake effect; only covering a small part of El Puntal and Somo beach (the wave energy reduction is seen on approximately 1 km of coastline); but for the same reason the wave energy reduction is higher, reaching values of 20–25%.

As stated before, the most common incident waves in Santander Bay correspond to case S2. For these waves the Wave Dragon reduces by almost 15% the wave energy that arrives at the output line in front of Somo beach. In turn, Sardinero beach, Magdalena peninsula and El Puntal are naturally protected with this wave condition, giving a favourable performance for this apparently small farm. As for the Blow-Jet, very low energy reduction is found and only a small section in front of Loredo beach sees wave energy reduction.

The above can be further understood if the local to incident wave ratios along the output line for unprotected, WD and BJ wave fields are compared, thus evaluating the wave height reduction near-shore due to the WECs. To compute this ratio, the propagated wave heights along the 5 m depth line (see output line in Fig. 7) have been taken from El Puntal to Loredo beach for the four modelled scenarios. The results are presented in Fig. 14, where H stands for wave height and the subscripts L and 0 for local and incident, respectively. As mentioned earlier, for case S1, the West of Somo beach is the best protected area (higher wave energy reduction in the output line), while Loredo and El Puntal receive low benefit from the devices, furthermore, in the interval 1800–2000 m of the output line (close to Somo beach), the WD farm produces higher waves than the unprotected case, mainly because of wave diffraction which produces a different distribution of the wave energy. For these S1 waves almost all the analysed beach fronts show very

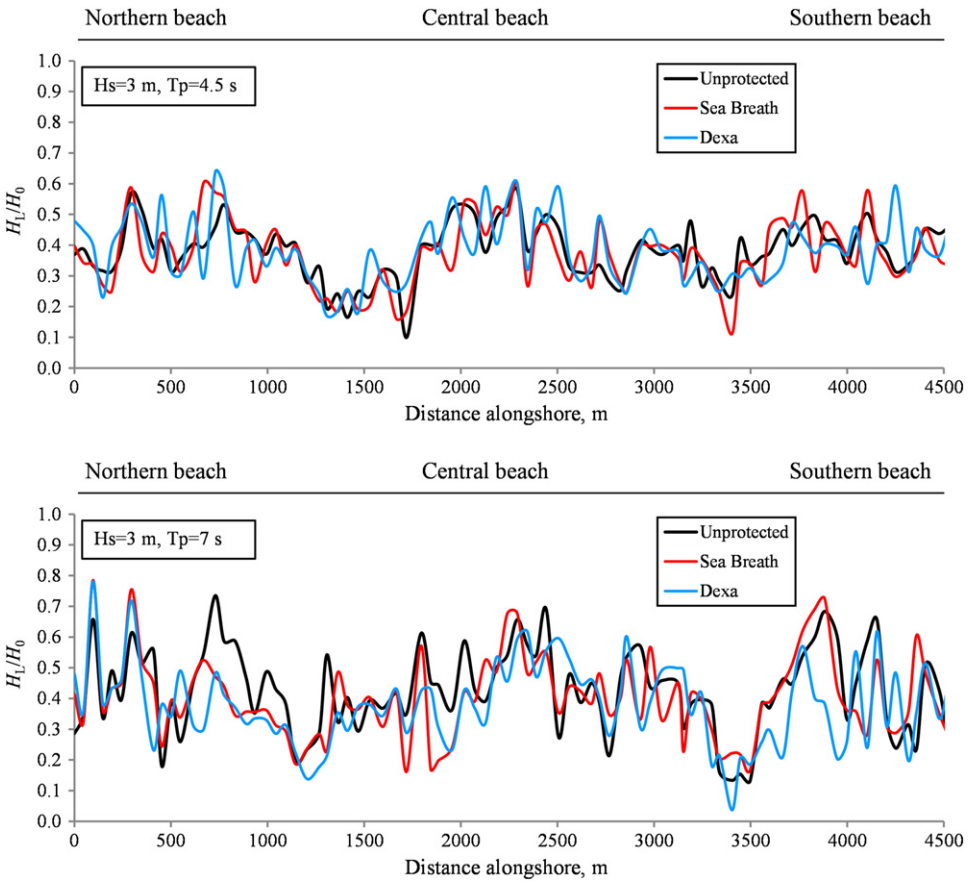

Fig. 16. Wave height reduction nearshore for Las Glorias beach, case G1 (top) and case G2 (bottom).

similar alongshore wave height distribution with and without the protection; nevertheless the overall performance is best for the farm placed in deeper waters.

Case S2 shows better overall performance of the Blow-Jet farm; it reduces wave energy at Somo beach and to a lesser extent at Loredo beach. As can be seen in Fig. 14 (bottom), the Wave Dragon farm practically does not reduce wave energy at Somo beach but significant reduction is found at Loredo beach.

4.3. Hydrodynamic performance in Las Glorias Beach

The numerical domain of Las Glorias Beach implemented in WAPOQP consisted of a regular grid of squared 5 m cells. The domain was rotated 23° counter clockwise to align the bottom boundary of the mesh with the bathymetric lines which is the hypothesis of the forcing boundary in any mild-slope model. Fig. 9 shows the rotated domain.

The case study at Las Glorias beach is of two devices with higher transmission coefficients per device, therefore the farms occupy a larger marine area. The wave periods that best fit the developing concept of these devices are short, which works in favour of their performance as coastal protection alternatives. The results of the wave fields imposed by these WEC farms are shown in Fig. 15.

In Fig. 15 the wake effect behind the Dexa is noticeable; even though the energy reduction is moderate it is of benefit to the North and Central beaches. The Seabreath also reduces wave energy to the North and Central beaches but in lower magnitude. The width of the wake effect of both farms covers approximately 2 km of coastline. In contrast to what one would expect, both farms seem to have higher energy absorption with the larger period (G2). Probably, in the case of Dexa, due to the large number of lines and, in the case of Seabreath, due to the narrow gaps; it has to be considered that G2 conditions were the ones selected to design and optimise the farms. Also in both farms the interaction of the waves with the sea bottom generates an energy concentration at the South that none of the farms is capable of dissipating. This and the possibility of designing the farms aligned to the wave direction, instead of the coastline, are objects for further investigation.

The detailed wave height reduction near-shore was studied for the whole beach front confirming the above finds. For the G1 case (Fig. 16, top) the protection given by the farms is small; in fact, in some areas the wave heights seem to be higher with the farms in place than in the present condition; as was said earlier this is due to the wave diffraction as it is the predominant physical phenomenon responsible of the energy distribution patterns when waves find an obstacle. The wave height distribution alongshore is similar for the three simulations.

For case G2 the wave energy reduction induced by the farms is greater in the North beach than in the Central beach. The overall efficiency is better for the farm with more lines.

5. Coastline response to WEC protection

The evaluation of the coastline response was performed in two steps: first the Long-shore Sediment Transport (LST) was computed and then the continuity of sediment equation was used to estimate the coastline evolution tendency.

The LST was computed using the Kamphuis (1991) equation as improved by Mil-Homens et al. (2013), that is

$$Q_l = 17.5 H_{sb}^{2.75} T_p^{0.89} m_b^{0.86} D_{50}^{-0.69} \sin^{0.5}(2\alpha_b) \quad (6)$$

where Q_l is the LST volume rate (m^3/s), H_{sb} the breaking wave height, T_p the period, m_b the beach slope, D_{50} the mean grain diameter and α_b the wave angle at the breaking point. The wave data were taken from the

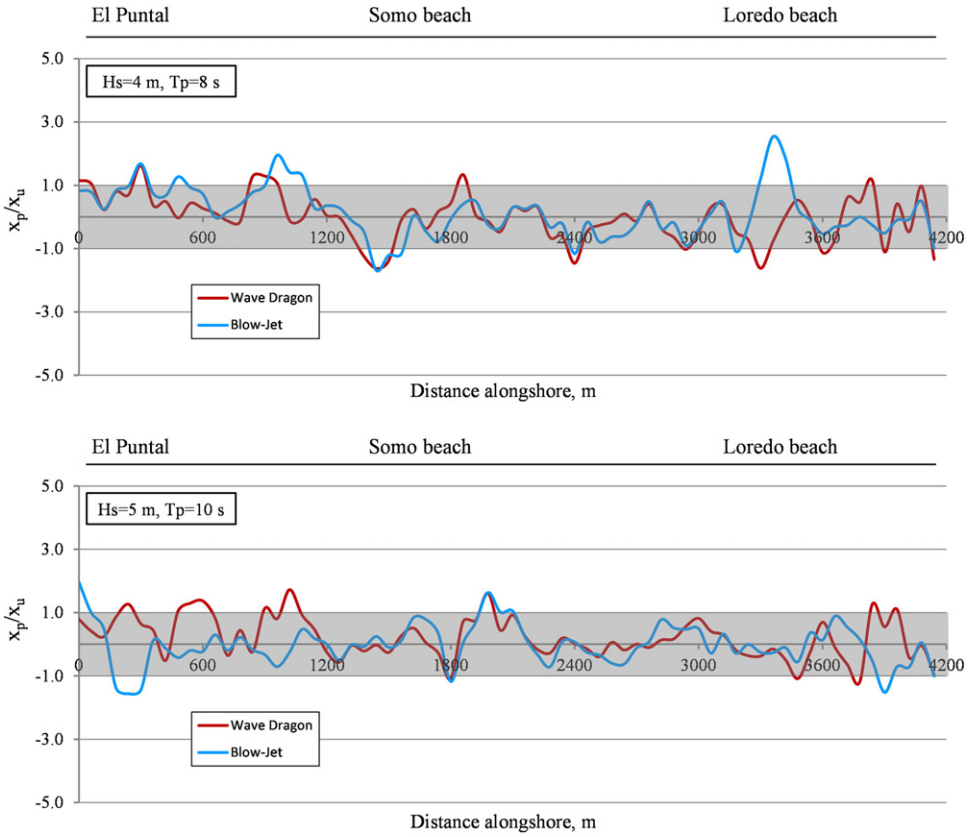

Fig. 17. Coastline evolution trends for Santander beaches; case S1 (top) and case S2 (bottom).

WAPOQP results; this gives the advantage of considering, from wave propagation, the effects of diffraction and refraction in the LST. The beach slope was taken directly from the bathymetry (0.02 for Santander and 0.01 for Las Glorias) and for the mean grain diameter values of 0.3 mm for Santander and 0.2 mm for Las Glorias (Medellin et al., 2008; Zayas, 2012, respectively) were used.

The LST values were used as input to the continuity of sediment equation, that is

$$\frac{\partial x}{\partial t}+\frac{1}{D_s}\left(\frac{\partial Q_l}{\partial y}-q\right)=0 \tag{7}$$

where x is the coastline position in the cross shore direction, D_s the closure depth, y the longshore axis and q any source or sink of sediment different to the LST. The result of Eq. (7) is the trend of the coastline movement. A full application of Eq. (7) requires a process of model calibration. Since measured historical data are unavailable for the study sites, the coastline tendency is evaluated as the ratio of the beach response induced by the WEC farms, x_p, to the present beach response, x_u. By taking the present position of the coastline as the reference position, the positive and negative values obtained from Eq. (6) mean, respectively beach tendency to accretion and erosion.

5.1. Coastline response in Santander Bay

The top panel of Fig. 17 shows the relative trend of Santander beaches with waves of S1 case. The coastline in which the Wave Dragon farm is reducing wave energy is evident at El Puntal and at the West of Somo beach where the tendency is of beach growth. In accordance with what was found in Section 3, Loredo beach was poorly protected by the Wave Dragon with S1 waves. The Blow-Jet is only capable of producing an accretive evolution trend at El Puntal and in a small portion of Loredo beach. The shadowed area in Fig. 17 (1.0 to −1.0 range of the x_p to x_u ratio) shows the coastline portions where the erosion or growth tendency is lower with the farms placed than in the actual scenario.

The G2 scenario for the coastline response in Santander Bay is shown in the bottom panel of Fig. 17 where it can be seen that the wave Dragon farm produces an accretive tendency for almost all the output line; the effect is low in magnitude but the protection objective is fulfilled. With these G2 case waves the Blow-Jet farm produces a positive (accretion) effect in a small portion of Somo beach and negative (erosion) trend at Loredo beach. In Fig. 17 it is verified the find that farms placed offshore reduce energy to a lesser extent than nearshore placed devices.

5.2. Coastline response in Las Glorias Beach

Fig. 18 presents the evolution trends of Las Glorias beach. In the upper panel case G1 is shown, where it can be seen that both farms (Dexa and Seabreath) have accretive effects in the North and Central beaches. The farm with fewer device lines produces a more accretive response, but shows a negative (erosion) effect in the part of the beach that is not protected, while the Dexa farm produces a more homogeneous response alongshore.

The accretion tendency induced by the Seabreath farm in case G2 is again moderate but homogeneous as in case G1, while the Dexa farm induces an accretive tendency in a short part of the Central beach (see the bottom panel of Fig. 18). For both farms a small negative effect is seen in the Central beach and the erosion response induced to the South beach is lower than for G1 waves. Although in Section 3 it was found that the energy reduction was greater in case G2, the accretive response is a little lower than the one found for case G1.

6. Conclusions

A numerical evaluation was performed on the effect of four WECs placed at two different sites, a semi-closed water body

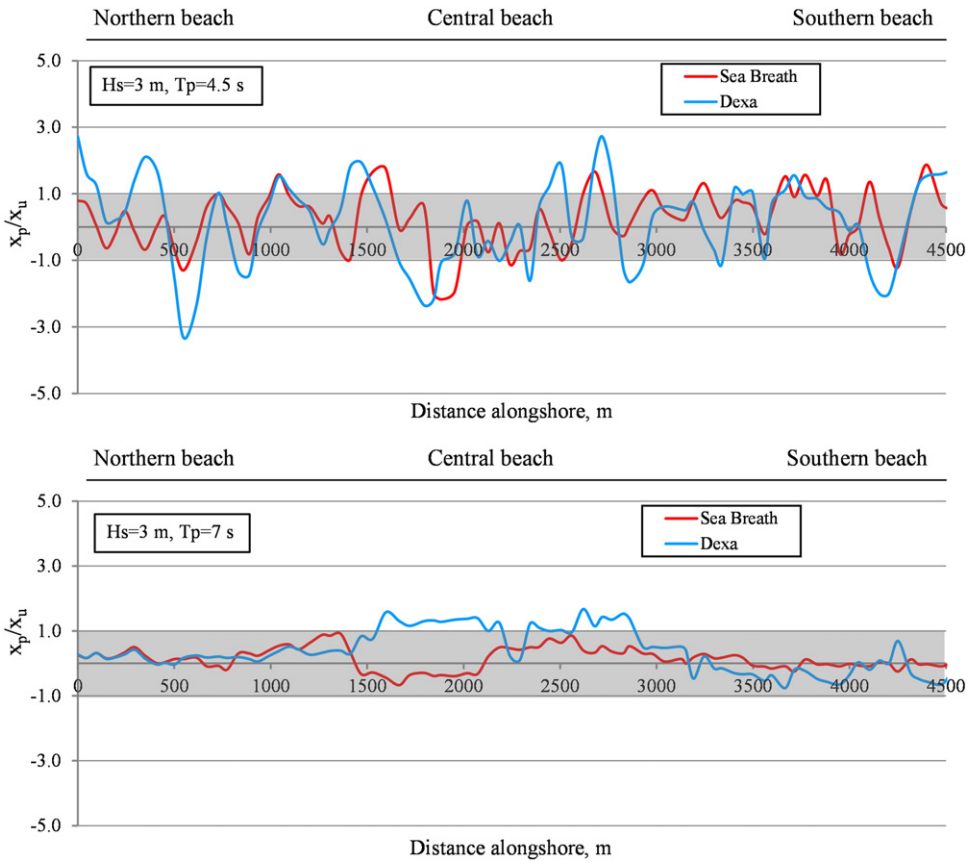

Fig. 18. Coastline evolution trends for Las Glorias beach; case G1 (top) and case G2 (bottom).

and an open beach. The wave field imposed by the devices was evaluated and used as an input for the LST calculation. Then the continuity of sediment equation was used to estimate the trends of coastline movement derived from the presence of the floating structures.

From the modelling of the Santander case it can be said that the selection of the device for shore protection is a combination of more variables than in the case of an open beach. If the length of coastline to be protected is large, then the device should be placed in deeper waters but the waves will have space enough to reset and gain some energy (from wind and shoaling), reducing the efficiency of the device. If low transmission coefficients or high wave reduction are needed, a device placed closer to the beach should be selected. To cover large areas, larger farms should be designed. The limitations to the size of the farms include coastal activities and navigation routes. It is also important to note that if the LST patterns are strongly modified, unexpected undesirable effects can result, e.g. the stability of El Puntal (sand spit) depends on the LST and strong alterations may weaken it.

La Glorias beach case study concludes that occupying more marine area does not necessarily mean a higher wake effect or wave energy reduction, nor better beach protection, but other marine activities, like fishing and navigation, can be affected by large WEC farms. The selection of the device in mild slope sites should be made very carefully as the distance of the farm from the coast is large and efficiencies can be dramatically reduced. It is recommended to select devices with shorter longshore gaps if the length to be protected is large, and farms with more lines where high wave reduction is needed in short lengths. It is also important to point out that a farm with several lines tends to behave as a nearshore farm.

It is clear that greater shore protection could have been achieved with traditional alternatives, but then only this goal would have been fulfilled and no other benefit would be obtained. The advantage of the WEC farms is that they provide two services and are, as has been said throughout this paper, an alternative; so if the protection offered by the farm is in agreement with the use of the beaches, then the alternative is feasible. The ultimate decision depends on coastal management.

Notations

D_{50}	sediment mean diameter, mm
D_s	closure depth, m
E	porosity
F	friction coefficient
H_0	incident wave height, m
H_L	local (propagated) wave height, m
H_{sb}	wave height at breaking point, m
$K_{T,D}$	transmission coefficient for a single device
K_T	empirical transmission coefficient for Seabreath 1:100 scale tests
L_p	deep water peak period wave length, m
m_b	beach slope from coastline to breaking point
P	device draught, m
Q_l	LST rate, m^3/s
T	wave period, s
W	device longshore width, m
x_p	beach response trend value with WEC farms in place, m
x_u	beach response trend value without WEC farms, m
α_b	wave direction at breaking point, degrees
θ	incident wave direction, degrees

Acknowledgements

The support of the European Commission through FP7.2009-1, Contract 244104—THESEUS project ("Innovative technologies for safer European coasts in a changing climate"), www.theseusproject.eu, is gratefully acknowledged.

The authors are very grateful to all the researchers involved in the development of this paper and the results presented in it, in particular to Xavier Chávez for his technical support.

References

Angelelli, E., Zanuttigh, B., 2012. A farm of wave activated bodies for coastal protection purposes. Proc. 33rd International Conference on Coastal Engineering, Santander, ES.
Babarit, A., 2013. On the park effect in arrays of oscillating wave energy converters. Renew. Energy 58, 68–78.
Beels, C., Troch, P., De Backer, G., Vantorre, M., De Rouck, J., 2010a. Numerical implementation & sensitivity analysis of a wave energy converter in a time-dependent mild-slope equation model. Coast. Eng. 57 (5), 471–492.
Beels, C., Troch, P., Visch, K.D., Kofoed, J.P., Backer, G.D., 2010b. Application of the time-dependent mild-slope equations for the simulation of wake effects in the lee of a farm of wave dragon wave energy converters. Renew. Energy 35 (8).
Beels, C., Troch, P., Kofoed, J.P., Frigaard, P., Kringelum, J.V., Kromann, P.C., Donovan, M.H., De Rouck, J., De Backer, G., 2011. A methodology for production and cost assessment of a farm of wave energy converters. Renew. Energy 36 (12), 3402–3416.
Borgarino, B., Babarit, A., Ferrant, P., 2011. Impact of wave interactions effect on energy absorption in large arrays of wave energy converters. Ocean Eng. 41, 79–88.
Budal, K., 1977. Theory of absorption of wave power by a system of interacting bodies. J. Ship Res. 21, 248–253.
Child, B., Venugopal, V., 2007. Interaction of waves with an array of floating wave energy devices. Proc. of the 7th European wave and tidal energy conference, Porto, Portugal.
Evans, D.V., 1979. Some theoretical aspects of three dimensional wave energy absorbers. Proc. of the 1st symposium on wave energy utilization, Gothenburg, Sweden.
Falnes, J., 1980. Radiation impedance matrix and optimum power absorption for interacting oscillators in surface waves. Appl. Ocean Res. 2, 75–80.
Folley, M., Whittaker, T., 2010. Spectral modelling of wave energy converters. Coast. Eng. 57 (10), 892–897.
Folley, M., Babarit, A., Child, B., Forehand, D., O' Boyle, L., Silverthorne, K., Spinneken, J., Stratigaki, V., Torch, P., 2012. A review of numerical modeling of wave energy converter arrays. Proceedings of the 31st International Conference on Ocean, Offshore and Arctic Engineering, Rio de Janeiro, Brazil, pp. 1–11.
Garnaud, X., Mei, C.C., 2009. Bragg scattering and wave-power extraction by an array of small buoys. Proc. Roy. Soc. A Math. Phys. Eng. Sci. 466, 79–106.
Kamphuis, J.W., 1991. Alongshore sediment transport rate. J. Waterw. Port Coast. Ocean Eng. 1170 (6), 624.
Kofoed, J.P., 2009. Hydraulic evaluation of the DEXA wave energy converter. DCE contract report No. 57. Dep. of Civil Eng. Aalborg University.
Li, Y., Yu, Y.H., 2012. A synthesis of numerical methods for modeling wave energy converter-point absorbers. Renew. Sustain. Energy Rev. 16 (6), 4352–4364.
Medellin, G., Medina, R., Falqués, A., González, M., 2008. Coastline sand waves on a low-energy beach at "El Puntal" spit, Spain. Mar. Geol. 250 (3–4), 143–156.
Mendes, L., Palha, A., Fortes, C.J., Brito-Melo, A., Sarmento, A., 2008. Analysis of the impact of a pilot zone for wave energy conversion offshore Portugal. Proc. Of the 18th International Offshore and Polar Engineering Conference (401 pp.).
Mil-Homens, J., Ranasinghe, R., van Thiel de Vries, J.S.M., Stive, M.F.J., 2013. Re-evaluation and improvement of three commonly used bulk longshore sediment transport formulas. Coast. Eng. 75, 29–39.
Millar, D.L., Smith, H.C.M., Reeve, D., 2007. Modelling analysis of the sensitivity of shoreline change to a wave farm. Ocean Eng. 34, 884–901.
Nørgaard, J.H., Lykke Andersen, T., 2012. Experimental and numerical investigation of wave transmission from a floating wave dragon wave energy converter. International Ocean and Polar Engineering Conference, Rhodes (ISOPE).
Ricci, P., Saulnier, J.B., Falcão, A.F. de O., 2007. Point-absorber arrays: a configuration study off the Portuguese West-Coast. Proc. of the 7th European wave and tidal energy conference, Porto, Portugal.
Ruol, P., Martinelli, L., Pezzutto, P., 2011a. Multi-chamber OWC devices to reduce and convert wave energy in harbour entrance and inner channels. Proc. of the Twenty-first International Offshore and Polar Engineering Conference (ISOPE) Maui, Hawaii, USA, June 19–24(2011), pp. 622–629.
Ruol, P., Zanuttigh, B., Kofoed, J.P., Martinelli, L., Frigaard, P., 2011b. Near-shore floating wave energy converters: benefits for coastal protection. Proc. ICCE No. 32(2010), Shanghai, China. Paper #: structures 6.1 (http://journals.tdl.org/ICCE/).
Silva, R., Salles, P., Palacio, A., 2002. Linear waves propagating over a rapidly varying finite porous bed. Coast. Eng. 44 (3), 239–260.
Silva, R., Mendoza, E., Losada, M.A., 2006. Modelling linear wave transformation induced by dissipative structures—regular waves. Ocean Eng. 33 (16), 2150–2173.
Silva, R., et al., 2008. Atlas de Clima Marítimo de la Vertiente Pacífica Mexicana. Universidad Nacional Autónoma de México.
Thorpe, T.W., 2000. Wave energy for the 21st century. Renewable Energy World, 7/8.
Van der Meer, J.W., Briganti, R., Zanuttigh, B., Wang, B., 2005. Wave transmission and reflection at low crested structures: design formulae, oblique wave attack and spectral change. Coast. Eng. 52 (10–11), 915–929.
Venugopal, V., Smith, G.H., 2007. Wave climate investigation for an array of wave power devices. Proc. of the 7th European wave and tidal energy conference, Porto, Portugal.
Zanuttigh, B., Martinelli, L., Castagnetti, M., Ruol, P., Kofoed, J.P., Frigaard, P., 2010. Integration of wave energy converters into coastal protection schemes. 3rd International Conference on Ocean Energy (ICOE), Bilbao.
Zanuttigh, B., Angelelli, E., Kofoed, J.P., 2013. Effects of mooring systems on the performance of a wave activated body energy converter. Renew. Energy 57 (9), 422–431.
Zayas, M., 2012. Effects of the construction of a groin, which alters the littoral transport on Las Glorias beach. MSc Thesis IPN (126 pp. (in Spanish)).